URC97160

Closed-Loop Aeromaneuvering for a Mars Precision Landing

Roy Smith
Electrical & Computer Engineering Dept.
University of California, Santa Barbara
Santa Barabara, CA 93106

Dhemetrios Boussalis and Fred Y. Hadaegh
Jet Propulsion Laboratory
California Institute of Technology
Pasadena, CA 91109

Abstract

Controlled aeromaneuvering is considered as a means of achieving a precisely targeted landing on Mars. This paper presents a preliminary study of the control issues. The candidate vehicle is the existing Mars Pathfinder augmented with roll thrusters and a center of mass offset actuator. These allow control of both bank angle and lift force, giving the ability to control the range and cross-track during the aeromaneuvering entry. A preliminary control system structure is proposed and a design simulation illustrates significant targeting improvement under closed-loop control.

1 Introduction

This paper describes on-going work on the development of technologies needed for precision landings on Mars, The current Mars Pathfinder mission uses a small bluff vehicle on a ballistic trajectory. The error in specified landing position is an ellipse of approximately 300 km by 150 km.

The objective of this work is to develop the feedback control strategies necessary to reduce this error ellipse to less than 10 km, and, in the longer term, to less than 1 km. This level of precision will enable targeting for specialized science missions; for example: landing inside a crater of 20 km in diameter; or retrieving samples from a prior mission.

The major sources of landing error are navigation errors on the approach to atmospheric entry, and, more critically, uncertainties in the atmospheric properties. In order to reduce these errors it is necessary to use closed-loop feedback control during the atmospheric entry phase. The cent rolled aeromaneuvering issues are discussed in this paper. The complete mission will also involve parachute and terminal landing phases. Work on these phases is in the preliminary stages and is not discussed in detail here.

The candidate landing vehicle is based on the existing Pathfinder entry vehicle. This is a low lift vehicle, with maximum lift to drag ratio of less than 0.3, which imposes limitations on the control design problem. The advantages of using this vehicle are low development cost and access to an existing aerodynamic database. In its nominal configuration the Pathfinder vehicle generates no lift. We are proposing that a variable center of mass offset be used as an actuator to generate a controlled lift force and that roll thrusters be used to bank and thereby steer the vehicle.

1.1 Mission Scenario

This study considers the case where the atmospheric entry is made directly from interplanetary cruise, rather than first going into orbit. This is more appropriate for a small low cost mission, and gives a higher entry velocity. It does not consider the potential for reducing the navigational errors during an orbital phase.

The descent to landing consists of three phases: atmospheric aeromaneuvering; parachute; and terminal landing phase. The atmospheric entry phase begin at an altitude of 125 km when the vehicle has a velocity, V, of 7.5 km/second. The flight path angle, γ, is nominally -14.2 degrees. The parachute is deployed at an altitude of 8 to 10 km, when the velocity has decelerated to approximately 0.5 km/see. At the parachute deployment the fright path angle is between -45 and -60 degrees. The parachute is released at an altitude of approximately 5 km, when the velocity has further decelerated to 60 m/see. A three axis reaction control system (RCS) is then used to navigate and descend to a soft landing.

The work described here considers only the aeromaneuvering control aspect of this problem. The entry into the upper atmosphere is considered as the initial point for this control. The objective is to control the atmospheric descent and guide the vehicle to the start of the parachute phase above a prespecified target on the planet.

The 1997 Pathfinder mission to Mars will use a bluff body on a ballistic entry trajectory. The errors in the atmospheric entry conditions (flight path angle, azimuth angle, and entry altitude) and uncertainties in the atmospheric properties and vehicle aerodynamics translate to a target accuracy of approximately 300 km by 100 km.

The objective of this work is to used closed-loop control during the atmospheric entry phase to reduce the error at parachute deployment to within 10 km or less. The controlled terminal phase will further reduce this error, with the longer term design objective being a total system landing error under 1 km.

1.2 Related work

Controlled aeromaneuvering has been considered in a number of other applications, Lifting trajectories have been used in the Apollo, Shuttle and Viking programs. See Dierlam [1], and the references therein, for more detail on the strategies used in these cases. Although the Viking program placed vehicles on Mars, these were not precision landings [2]. An open-loop strategy was used and the 3-σ ellipse was of the order of 120 km x 60 km. The Apollo program used a low L/D ratio (0.3) vehicle and bank angle control to maintain a reference drag profile. Crossrange requirements were met by changing the sign oft he bank angle in response to current crossrange error. The desired landing accuracy was 15 nautical miles.

The Shuttle program uses a vehicle with an approximate L/D ratio of 1.2 and has significantly greater accuracy requirements. Control is implemented via bank angle, angle-of-attack and a speed brake, which are used to fly reference drag and altitude rate profiles. In the case of Earth re-entry a better characterization of the atmosphere is available, reducing the uncertainty associated with the problem. In this case the entry conditions can also be more precisely specified.

Dierlam [1] describes a simulation study of a bank angle control strategy for landing a vehicle on Mars. A predictor-corrector strategy is used to predict the terminal errors which result from the currently estimated trajectory errors and forms the basis of the control algorithm. This work is similar in several respects although it considers a three degree of freedom simulation and does not consider the effects of uncertainty on vehicle orientation. The use of a predictor-corrector based guidance algorithm for aerobraking in the Martian atmosphere has been considered by Braun and Powell [3].

2 Vehicle Characteristics

The candidate vehicle is based on the Pathfinder aeroshell design, depicted in Figure 1. Detailed aerodynamic and configuration information is available in the work of Spencer and Braun [4], The vehicle studied here is augmented with two control actuators. The first is a variable center of mass offset, and is used to alter the trim angle-of-attack and thereby generate lift. The second is a pair of thrusters used to roll the vehicle, and thereby steer the lift force.

The prior work on the aerodynamic properties of the Pathfinder aeroshell [4] assumes a trim angle-of-attack, α, of zero which is the case for ballistic entry trajectories. We consider using a variable center of mass offset as an actuator, which necessitates developing an aerodynamic model for other values of α. This approach is based on a Newtonian impact theory model. This model is appropriate for the hypersonic entry considered here, and we also use it as an approximate ion for lower velocities closer to the planet surface. Future work will require the development of more detailed aerodynamic models for the lower velocities,

The lift and drag forces acting on the vehicle are given by, $L = QSC_L$ and $D = QSC_D$, where S is a reference area (in this case 5.515 m^2) and Q is the dynamic pressure, given by, Q = $\rho V^2/2$. The atmospheric density is ρ, and V is the vehicle velocity. The lift and drag coefficients, C_L and C_D, are function of the angle-of-at tack, α, and the side-slip angle, β. Because of the circular symmetry of the aeroshell we can combine α and β into a single effective angle of attack variable, a,, defined by

$$\sin^2\alpha_e = \cos^2\beta \sin^2\alpha + \sin^2\beta.$$

This is effectively the angle-of-attack in a frame rotated by an angle,

$$6' = \arctan\left(\frac{-\cos\alpha\sin\beta}{\sin\alpha}\right),$$

with respect to the wind frame. In this frame the lift and drag coefficients can be approximated by,

$$C_L = C_N\cos\alpha_e - C_A\sin\alpha_e \qquad \text{and} \qquad C_D = C_N\sin\alpha_e + C_A\cos\alpha_e,$$

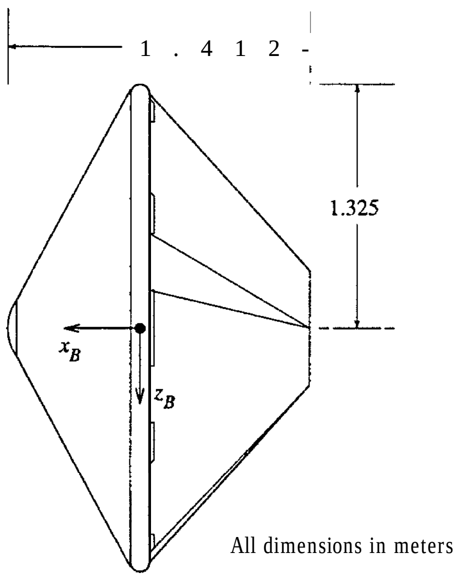

Mass (kg)	552.0			
Inertias	(kg.m^2)	I_x	I_y	I_z
		230.0	184.0	180.0
		I_{yz}	I_{xy}	I_{zx}
		0.0	0.0	0.0

Figure 1: Pathfinder entry vehicle configuration

where C_N and CA are the normal and axial coefficients, which are approximated by,

$$C_N = 0.4381\alpha_e \quad \text{and} \quad C_A = 1.7204 - 1.5623\alpha_e^2.$$

The pitching and yawing moments are given by, $M = QcSC_m$ and $N = QbSC_n$, where b and c are reference lengths, which are both 1.325 m in this case. These moment equations determine the static trim of the vehicle. In the standard configuration this is $\alpha = 0$, $\beta = 0$. The actuation considered here involves offsetting the center of mass in the body Z axis, by an amount dz. With this offset the coefficients are,

$$C_m = C_{moz}dz + C_{ma}\alpha + C_{mq}q \quad \text{and} \quad C_n = -C_{ma}\beta + C_{nr}r,$$

where q is the pitch rate and r is the yaw rate. The coefficients are $C_{moz} = 1.6757$, $C_{ma} = -0.5275$, $C_{mq} = -0.05$, and $C_{nr} = -0.054$. Note that the Z axis center of mass offset does not affect the yaw moment. These Figure 2a) illustrates C_m and C_n as a function of α and β. This figure can be interpreted by considering the velocity vector as pointing directly at the viewer from the origin. The stem of each arrow is placed on the vehicle nose and the arrow then gives the relative size and direction of the corresponding moment acting on the vehicle. The figure shows $dz = -0.099$ which gives a static trim of $\alpha = -18.0$ degrees (sin $\alpha = -0.309$). This is the maximum magnitude trim angle and gives a maximum lift coefficient of $C_L = 0.3531$ and a lift/drag ratio of 0.2305.

The achievable range is illustrated in Figure 2b). The entry trajectories are illustrated for the maximum and minimum angles-of-attack. This corresponds to a movement of the center of mass of $\pm 7\%$ of the vehicle radius. The resulting ground track is extended over 800 km beyond the ballistic case. Varying the center of mass offset, dz, allows control actuation over this range.

3 Control Issues

The two major sources of error are navigation errors at entry and atmospheric uncertainty. The most significant entry condition errors are in altitude (± 2.5 km) and flight path angle (+1.0 degrees). The knowledge error associated with these is an order of magnitude less which gives the potential to correct for these errors during the aeromaneuvering phase. This work uses a simple exponential model for the Martian atmospheric density,

$$p = \rho_r e^{-0.1(R-R_r)}, \quad R_r = 3,4290.0 \text{ km}, \quad \rho_r = 7.8 \times 10^5 \text{kg/km}^3,$$

as a function of altitude, R, expressed as a radius from the planet center. The uncertainty in atmospheric density considered in this work is $\pm 25\%$.

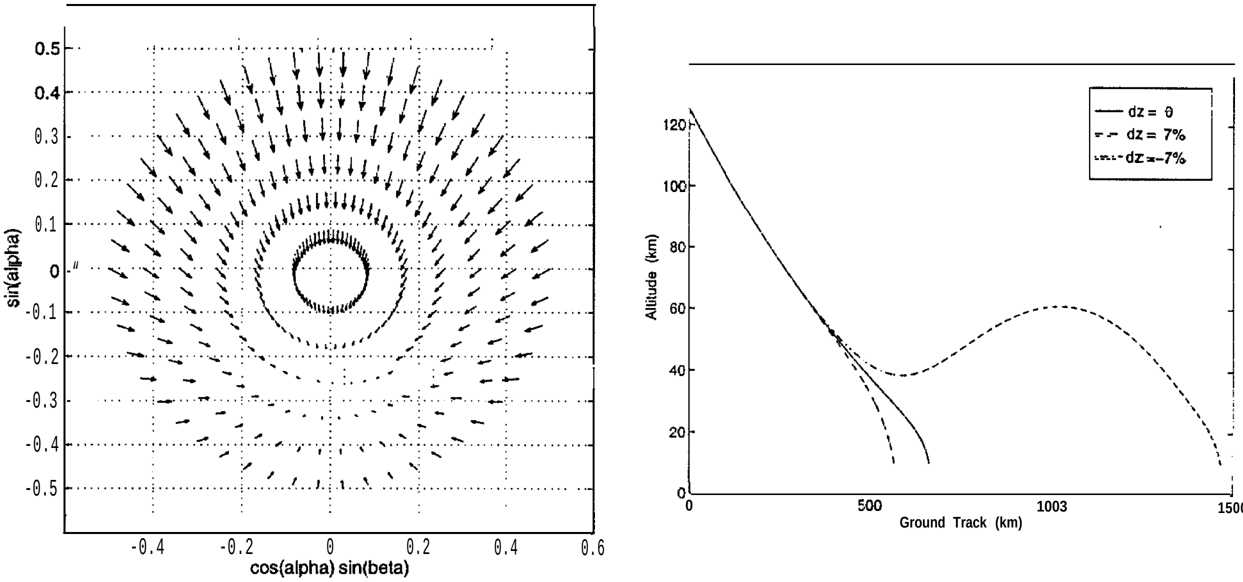

a) b)

Figure 2: CM actuated vehicle: a) Pitch/ yaw moments. b) Trajectories for α = +18, O, -18 degrees

A more significant control issue is the nonlinearity in the control actuation. As illustrated previously, the lift force can be controlled by moving the center of mass. The actuator effectiveness is directly proportional to the dynamic pressure, Q. Figure 3 illustrates the lift and drag forces that result from a nominal trajectory of $\alpha = -13$ degrees.

At the atmospheric entry (t = 0), the density is so small that Q is effectively zero. As the density increases the V^2 term causes a rapid increase in Q. The vehicle decelerates quickly, causing Q to drop to a low level for the duration of the entry. There is a window of maximum effective control opportunity between t = 50 and t = 100 seconds. Only limited control capability is possible after t = 100 seconds. The vehicle position, in planet latitude and longitude, is very sensitive to both control actions and atmospheric perturbations occurring within that 50 second window.

To illustrate the nature of the system dynamics, we present a simplified set of dynamical equations for this problem. The velocity, V, is given by

$$\frac{dV}{dt} = \frac{-D}{m} - g \sin\gamma,$$

where g is the gravitational acceleration and m is the vehicle mass. The flight path angle, γ, equation is

$$V\frac{d\gamma}{dt} = \frac{L}{m} \cos\sigma - \left(g - \frac{V^2}{R}\right) \cos\gamma.$$

The azimuth/heading angle, ψ, is determined by,

$$V\frac{d\psi}{dt} = \frac{L}{m\cos\gamma} \sin\sigma - \frac{V^2}{r} \cos\gamma \cos\psi \tan\mu,$$

where μ is the longitude. The control system can influence the lift and drag (L and D above) by changing the center of mass offset, dz, and thereby changing α. The roll thrusters allow the controller to vary the bank angle, σ. Note that in the above equations all terms are actually functions of time. Not shown are the vehicle moment equations, or the equations determining vehicle position in planet centered coordinates.

4 Candidate Control Structure

Figure 4 illustrates the control structure considered for this problem. This consists of the following components.

Nominal Path. The nominal control actions, u_{nom}, are determined by an offline optimization. The issues that must be considered include: vehicle dynamics and maneuvering constraints; entry location

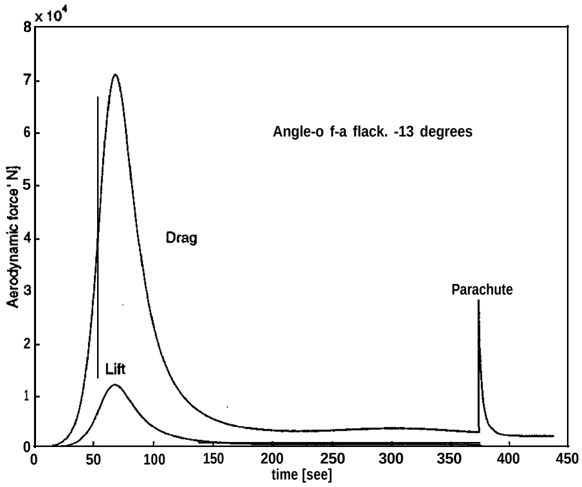

Figure 3: Lift and drag profiles

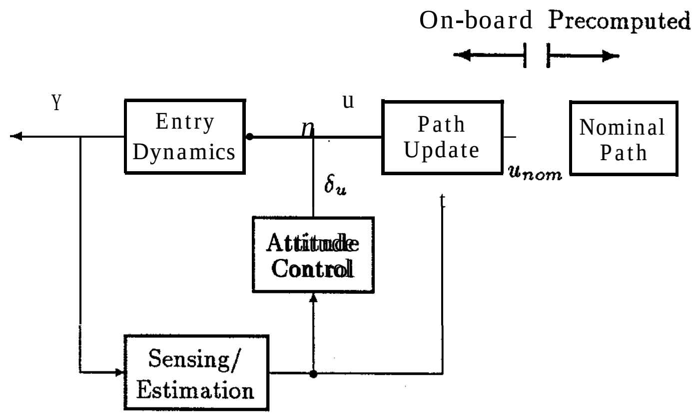

Figure 4: Control structure

and errors; control system achievable performance; atmospheric models; actuation saturation (rate and magnitude) constraints; terminal objectives (velocity, position, flight path angle); sensing limitations; robustness to system and atmospheric uncertainties; dynamic loading constraints; and thermal constraints.

Path Up date.' Trajectory deviations will be caused by entry condition errors and atmospheric perturbations and will require the calculation of a corrected trajectory. This involves a nonlinear prediction of terminal conditions based on the best current estimates of position, velocities, attitude and atmospheric variables, followed by a correction algorithm to determine the require control, u. Operational constraints (saturations, thermal limits, dynamic load limits) on the modified flight path must be considered. A sampled prediction/correction algorithm gives periodic up dates for u.

Attitude Control. Low level attitude control is required to fly the current modified flight path. The control input, u, is specified in terms of a (angle-of-attack) and σ (bank angle). A high bandwidth (continuous or digital) control law is required to generate the appropriate center of mass offset and roll thruster commands. A nonlinear/gain scheduled control is needed to account for widely varying vehicle response over the flight path.

Sensing/Estimation. The vehicle position, attitude and velocity is estimated from inertial measurement unit and any measurements (e.g. stagnation pressure). The parameters in atmospheric models, including density, are estimated and used for both attitude control and flight path updating. This is a highly nonlinear estimation problem, particularly for the atmospheric parameters. The quality of the velocity/attitude estimation is a function of IMU drift and will degrade over time. The quality of the atmospheric parameter estimates will improve over time.

5 Preliminary Design

A preliminary design has been evaluated and the results are shown graphically in Figure 5. The calculations involve a full 6 degree-of-freedom model. The primary reference for this type of model is Etkin [5], and for specific detail on the aeromaneuvering dynamic equations see Boussalis [6] and Smith [7].

The nominal trajectory was generated by selecting u_{nom} to be $\alpha = -13$ degrees and $\sigma =$ O degrees. These values take the vehicle to close to the center of its achievable range (refer to Figure 2b).

The path update used a predictor to estimate the terminal range as a function of α. This predictor used a nominal model for the atmospheric density. The prediction result was used to select a new value for α. The desired bank angle was generated by a tracking controller following a precalculated azimuth trajectory. The estimator design problem is currently being investigate ed in more detail. The preliminary y design shown here used a measurement of the vehicle velocity, position, and attitude. This is optimistic in that these values will be degraded in an estimator. However, the use of an estimator would also give the opportunity to use more accurate atmospheric density values. The exact nature of this trade-off will be investigated in future research.

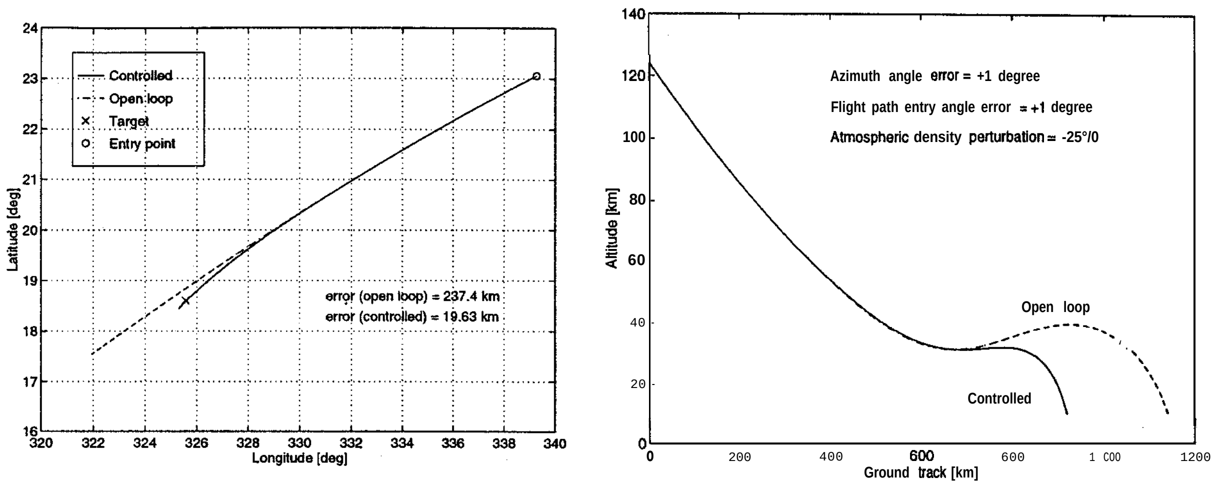

Figure 5: Simulated aeromaneuvering control system

The simulated entry conditions include a one degree error in both the azimuth and the flight path angle. In addition, the atmosphere was 25% less dense than the nominal case. Without closed-loop control, these conditions lead to a terminal landing error of 237 km. The closed-loop control reduces this error to under 20 km.

6 Summary

The simulation results indicate that controlled aeromaneuvering, using roll thrusters and center of mass offset actuation, has the potential to significantly reduce the landing error ellipse. On-going work is focusing on the development of higher performance controllers incorporating atmospheric density estimators. Overall system performance will be more extensively evaluated using more detailed models of system sensors, actuators, noise and drift. The attitude stabilization and RCS with optical sensing design problems will be studied for the parachute and terminal landing phases.

Acknowledgements

The research described in this paper has been performed at the Jet Propulsion Laboratory, California Institute of Technology, under contract with the National Aeronautics and Space Administration.

References

[1] T. A. Dierlam, "Entry Vehicle Performance Analysis and Atmospheric Guidance Algorithm for Precision Landing on Mars," 1990. MS Thesis, Massachusetts Institute of Technology.

[2] E. A. Euler, G. L. Adams, and F. W. Hopper, "Design and Reconstruction of the Viking Lander Descent Trajectories,)' *J. Guidance & Control, vol.* 1, September-October 1978.

[3] R. D. Braun and R. W. Powell, "Predictor-Corrector Guidance Algorithm for Use in High-Energy Aero-Braking Studies," *AIAA J. Guidance, Control* and Dynamics, vol. 15, pp. 672-678, May-June 1992.

[4] D. A. Spencer and R. D. Braun, "Mars Pathfinder Atmospheric Entry Trajectory Design," in *AAS/AIAA Astrodynamics Specialist Conf.*, August 1995. AAS Paper # 95-379.

[5] B. Etkin, *Dynamics of Atmospheric Flight,* Wiley & Sons, 1972.

[6] , "Investigation of the Longitudinal Motion of Low-Lift Entry Vehicles," Tech. Rep. EM 3456-96-002, Jet Propulsion Laboratory, May 1996.

[7] R. Smith, "Closed-Loop Aeromaneuvering for a Mars Precision Landing," Tech. Rep. Center for Control Engineering & Computation, University of California, Santa Barbara, Feb. 1996. CCEC-96-0205.